Energy conservation equations and interaction contributions at a structural interface between two dissipative media. Numerical experiments

Johana Brokešová, Vlastislav Červený

Charles University, Faculty of Mathematics and Physics, Department of Geophysics, Ke Karlovu 3, 121 16 Praha 2, Czech Republic, E-mails: johana@seis.karlov.mff.cuni.cz, vcerveny@seis.karlov.mff.cuni.cz

Summary

Energy conservation equations at a plane interface between two dissipative media are studied, assuming a plane elastic wave incident on it. In dissipative media, the conservation equations are more complex than in non-dissipative media. Among others, they contain the interaction contributions. The main purpose of this paper is to investigate numerically the energy conservation equations and the interaction contributions. An attempt is done to a find whether some energy-based quantities could be used in the local criteria for selection of proper "downgoing" and "upgoing" reflected and transmitted waves. The specification of downgoing and upgoing waves in dissipative media is not straightforward. For non-dissipative media, such energy-based criteria have been well known, but for dissipative media the general criteria have not yet been proposed. To make the numerical investigation more transparent, only the simplest reflection/transmission problem, corresponding to an SH incident wave, is considered. Numerical experiments offer certain interesting conclusions, but no one of these conclusions can be directly applied in the selection criteria. A suitable selection criterion is proposed for a special, but very important case, in which the angle of incidence equals the attenuation angle. The proposed selection criterion may be used quite safely both in isotropic and anisotropic media.

1 Introduction

In Červený (2001c), energy fluxes of plane elastic waves propagating in anisotropic dissipative media are investigated theoretically, particularly the complex-valued Poynting vector $\mathbf{F}$ (see Auld 1973; Ainslie and Burns 1995), the average energy flux $\mathbf{S}$ (Burridge 1976; Auld 1973) and the instantaneous energy flux $\mathbf{W}$ (Deschamps 1990; Ainslie and Burns 1995). Suitable expressions for energy fluxes of summary waves, consisting of several plane waves, are derived. These expressions, corresponding to the interaction of individual elementary waves, contain also interaction contributions. The derived equations are also used in the reflection/transmission problem at a structural interface, in the definition of energy-based R/T coefficients, in the formulation of energy conservation equations, and in the investigation of interaction contributions.

Seismic Waves in Complex 3-D Structures, Report 11 (Department of Geophysics, Charles University, Prague 2001)

In this article, we investigate all the derived equations and introduced quantities numerically. To make the investigation and conclusions more transparent, we consider only the simplest possible R/T problem, corresponding to the reflection and transmission of plane SH waves at a structural plane interface between two dissipative media.

The general R/T process at an interface between two dissipative elastic media is explained in Section 2, and for SH waves in Section 3. The selection criteria how to choose the downgoing and upgoing, reflected and transmitted waves, are discussed. A global selection criterion, based on the analytical continuation, is explained. It was used successfully by Krebes (1984), Brokešová and Červený (1998), and Brokešová (in press) to compute R/T coefficients. Such a criterion may be used both in dissipative and non-dissipative media. In non-dissipative media, however, the local energy-based criterion can be also used. It is based on the direction of the average energy flux. It is considerably more flexible than the global analytical continuation criterion. For dissipative media, a general local criterion has not yet been proposed.

In Section 4, the model for the computation is introduced, and the SH reflection coefficients are discussed. It is shown that the global criteria based on the analytical continuation and the local energy-based criteria do not always give the same result. Whereas the SH reflection coefficients are quite smooth if the global analytical continuation criterion is applied, they display sharp jumps if the local energy-based criterion is applied (at least in certain cases).

In Section 5, also some other energy fluxes are numerically studied, and their relation to the computation of the reflection/transmission coefficients is discussed. In Section 6, the energy conservation equations are investigated. It is shown that the energy conservation equations are satisfied not only if the global analytical criterion is used, but also if the local energy-based criterion is applied. Consequently, local energy-based selection criteria may be hardly based on the energy conservation equations.

In Section 7, a special, but very important case of the incident wave is considered, for which the angle of incidence equals the attenuation angle γ of the incident wave. In this case the attenuation vector is perpendicular to the interface, not only for the incident wave, but also for all generated R/T waves. The consequence is that the tangential components of the slowness vectors of the incident and all generated R/T waves are real-valued. A simple local selection criterion for reflected and transmitted waves can be then used, and the R/T coefficients can be evaluated without difficulties. This applies not only to isotropic, but also to anisotropic media, and to the reflection/transmission on a stack of homogeneous dissipative, isotropic or anisotropic, layers.

2 R/T problem on a plane interface between two dissipative media

We shall consider a plane interface Σ between two homogeneous isotropic or anisotropic, dissipative media, and a plane wave incident on it. We shall call the halfspace containing the incident wave the first halfspace, and the halfspace situated on the opposite side of the interface the second halfspace. We introduce the Cartesian coordinate system x_i with the x_3-axis perpendicular to Σ, pointing into the first halfspace. Thus the unit vector $\mathbf{n}$

normal to Σ has components (0,0,1).

In dissipative media, the slowness vectors $\mathbf{p}$ of individual waves (incident $\mathbf{p}^{inc}$, reflected $\mathbf{p}^{r}$, transmitted $\mathbf{p}^{t}$ are complex-valued,

$$p_k = P_k + \mathrm{i}A_k. \tag{1}$$

We shall call $\mathbf{P}$ the propagation vector, and $\mathbf{A}$ the attenuation vector. The propagation vector $\mathbf{P}$ shows the direction of propagation (perpendicular to the real-valued plane phase-front), and the attenuation vector $\mathbf{A}$ shows the direction of the steepest exponential decay of amplitudes. It is required that the angle γ between $\mathbf{P}$ and $\mathbf{A}$ satisfies the relation

$$-\frac{\pi}{2} < \gamma < \frac{\pi}{2}. \tag{2}$$

The angle γ is called the attenuation angle.

We assume that $\mathbf{P}^{inc}$ and $\mathbf{A}^{inc}$ are known for the incident wave. The determination of $\mathbf{P}^{r}$, $\mathbf{A}^{r}$ for reflected waves, and of $\mathbf{P}^{t}$, $\mathbf{A}^{t}$ for transmitted waves, is the basic procedure in the solution of the reflection/transmission problem. The tangential components of the slowness vectors of R/T waves can be determined simply. They equal the tangential components of the slowness vector of the incident wave

$$p_1^r = p_1^t = p_1^{inc}, \quad p_2^r = p_2^t = p_2^{inc}. \tag{3}$$

Equation (3) represents the complex-valued Snell's law for dissipative media. The determination of p_3^r and p_3^t (assuming that $p_1^r, p_2^r, p_1^t, p_2^t$ are known), is however considerably more involved. Let us consider, for a while, only the transmitted waves. (The treatment of reflected waves would be quite analogous.) Then the p_3-components can be determined as eigenvalues of a 6×6 matrix $\mathbf{A}$. (We have used the same symbol $\mathbf{A}$ also for the attenuation vector; we hope this will not cause any misunderstanding.) The explicit expressions for the 6×6 matrix $\mathbf{A}$ are given in Červený (2001b, Section 4), where also other references can be found. Matrix $\mathbf{A}$ has six eigenvalues, three correspond to downgoing and three other to upgoing waves. For transmitted waves, the three eigenvalues corresponding to downgoing waves should be selected. This would represent the complete solution of the problem. It is, however, necessary to specify strictly what we understand under downgoing and upgoing waves. To make the explanations more transparent, we shall first explain it on a simpler case, corresponding to the homogeneous incident wave in a non-dissipative medium.

In isotropic non-dissipative media, the eigenvalues can be found analytically, and the selection criterion is reduced to the choice of correct sign of $p_3 = [V^{-2} - p_1^2 - p_2^2]^{\frac{1}{2}}$, where V is the relevant velocity. For homogeneous transmitted waves, the sign is minus, as the transmitted waves are downgoing. For postcritical incidence, the transmitted wave is inhomogeneous, and p_3 imaginary valued. The correct sign is chosen in such a way to obtain an exponential decay of amplitudes of inhomogeneous transmitted waves from the interface.

For anisotropic non-dissipative media, the selection of p_3 is also straightforward. The eigenvalues, however, must be determined numerically. For any of six eigenvalues p_3, we have to determine the group velocity vector $\mathcal{U}$, mainly its normal component $\mathcal{U}_3$. The sign of $\mathcal{U}_3$ (not the sign of p_3) discriminates the downgoing and upgoing waves. Thus, for transmitted waves, $\mathcal{U}_3$ must be negative; the relevant component of the slowness vector p_3 may be, however, positive. For complex-valued p_3, the choice is again based on the requirement of the exponential decay of amplitudes of the inhomogeneous transmitted wave from the interface. See more details in Červený (2001a, Section 2.3.3).

Consequently, the selection criteria for non-dissipative media are simple. In dissipative media, however, the problem is more complex. Local criteria, similar to those for non-dissipative media, have not yet been proposed. For these reasons, global continuation criterion was used in the previous computation of R/T coefficients in dissipative media, see Krebes (1984), Brokešová and Červený (1998), Brokešová (in press). In actual computations of R/T coefficients, the continuation criterion was used only for isotropic media, assuming that the vectors $\mathbf{P}^{inc}$, $\mathbf{A}^{inc}$ and $\mathbf{n}$ are coplanar. The continuation criterion consists in the computation of the critical angle(s), and in the choice of the correct sign of p_3 according to the relation of actual angle of incidence to the known critical angle(s). For $\mathbf{P}^{inc}$, $\mathbf{A}^{inc}$ and $\mathbf{n}$ non-coplanar, and particularly for anisotropic media, such criterion would be very cumbersome. It would be useful to propose some local selection criterion even for dissipative media. Such criterion may be based on various forms of energy fluxes, on the energy conservation laws, on the direction of the exponential decay of amplitudes, etc. See Sections 5, 6, and 7.

3 Special case: SH waves

In the following, we shall discuss only a simple case of SH waves in isotropic media. Moreover, we shall assume that $\mathbf{P}^{inc}$, $\mathbf{A}^{inc}$ and $\mathbf{n}$ are coplanar. Then the analogous vectors are coplanar even for reflected and transmitted waves, see Brokešová and Červený (1998). We denote the complex-valued rigidity in the first halfspace by μ_1, and in the second halfspace by μ_2. The displacement R/T coefficients of SH waves are given by relations

$$R^{SH} = \frac{\mu_1 p_3^{inc} - \mu_2 p_3^t}{\mu_1 p_3^{inc} + \mu_2 p_3^t}, \quad T^{SH} = \frac{2\mu_1 p_3^{inc}}{\mu_1 p_3^{inc} + \mu_2 p_3^t}. \tag{4}$$

We denote the normal component of the complex-valued Poynting vector by $F_3 = \mathrm{Re}F_3 + \mathrm{i}\mathrm{Im}F_3$, the normal component of the instantaneous energy flux by $W_3 = \mathrm{Re}W_3 + \mathrm{i}\mathrm{Im}W_3$, and the normal component of the average energy flux by S_3 (where S_3 is real-valued). Then the expressions for F_3, W_3 and S_3, and for relevant energy conservation equations read, see Červený (2001c, Section 9):

a) **Complex Poynting vector.** The energy conservation equation for the complex Poynting vector reads:

$$F_3^{inc} + F_3^r + F_3^{int} - F_3^t = 0. \tag{5}$$

Here $F_3^{inc}, F_3^r, F_3^{int}$ and F_3^t are complex-valued, so that (5) represents two real valued equations. Individual expressions are given by relations:

$$\begin{aligned} F_3^{inc} &= \mu_1 p_3^{inc}, \\ F_3^r &= |R^{SH}|^2 \mu_1 p_3^r, \\ F_3^t &= |T^{SH}|^2 \mu_2 p_3^t, \\ F_3^{int} &= -2\mathrm{i}\mu_1 p_3^{inc} \mathrm{Im}(R^{SH}). \end{aligned} \tag{6}$$

Here F_3^{int} is the complex-valued interaction term, generated by the interaction of the incident wave with the reflected wave in the first halfspace.

b) **Instantaneous energy flux.** The energy conservation equation for the complex-valued instantaneous energy flux reads:

$$W_3^{inc} + W_3^r - W_3^t = 0. \tag{7}$$

Here W_3^{inc}, W_3^r and W_3^t are complex-valued, so that (7) represents two real valued equations. Individual expressions are given by relations:

$$\begin{aligned} W_3^{inc} &= \mu_1 p_3^{inc}, \\ W_3^r &= (R^{SH})^2 \mu_1 p_3^r, \\ W_3^t &= (T^{SH})^2 \mu_2 p_3^t, . \end{aligned} \tag{8}$$

There is no interaction term in the energy conservation equation (7) for the instantaneous energy flux. This is a general rule, valid even for instantaneous energy flux in anisotropic inhomogeneous media, see Červený (2001c).

c) **Average energy flux.** The energy conservation equation for the real-valued average energy flux reads:

$$S_3^{inc} + S_3^r + S_3^{int} - S_3^t = 0. \tag{9}$$

Here $S_3^{inc}, S_3^r, S_3^{int}$ and S_3^t are real-valued, and are given by the relations:

$$\begin{aligned} S_3^{inc} &= \mathrm{Re}(\mu_1 p_3^{inc}), \\ S_3^r &= |R^{SH}|^2 \mathrm{Re}(\mu_1 p_3^r), \\ S_3^t &= |T^{SH}|^2 \mathrm{Re}(\mu_2 p_3^t), \\ S_3^{int} &= 2\mathrm{Im}(\mu_1 p_3^{inc})\mathrm{Im}(R^{SH}). \end{aligned} \tag{10}$$

Note that the normal average energy flux is a real part of the normal complex-valued Poynting vector. It has the same direction as the normal component of the group velocity vector, $\mathcal{U}_3$. S_3^{int} is the real-valued interaction contribution, corresponding to the interaction of the incident wave with the reflected wave in the first halfspace.

4 Reflection/transmission SH coefficients

We shall consider the following MODEL1 of the interface:

$$\begin{aligned} &\rho_1 = 2.00 \text{ g cm}^{-3}, && \rho_2 = 2.10 \text{ g cm}^{-3}, \\ &\beta_1 = 1.50 \text{ km s}^{-1}, && \beta_2 = 2.25 \text{ km s}^{-1}, \\ &Q_1 = 12, && Q_2 = 21. \end{aligned}$$

Here ρ_I are densities, β_I are S velocities, and Q_I the quality factors in the first and second halfspace, respectively.

Figures 1 and 2 show the SH reflection coefficients for MODEL1.The numbers at curves show the attenuation angle γ of the incident wave, i.e. the angle γ between $\mathbf{P}^{inc}$ and $\mathbf{A}^{inc}$, with $-\frac{1}{2}\pi < \gamma < \frac{1}{2}\pi$. The angle γ is positive for $\mathbf{A}^{inc}$ oriented to the right from $\mathbf{P}^{inc}$. Thus, if γ is positive, the amplitudes of the incident wave decay exponentially to the right from $\mathbf{P}^{inc}$ (towards the interface Σ). Figure 1 shows the SH reflection coefficients computed with the help of the analytical continuation criterion, see Brokešová and Červený (1998). Figure 2 displays the SH reflection coefficients, computed with the help of the

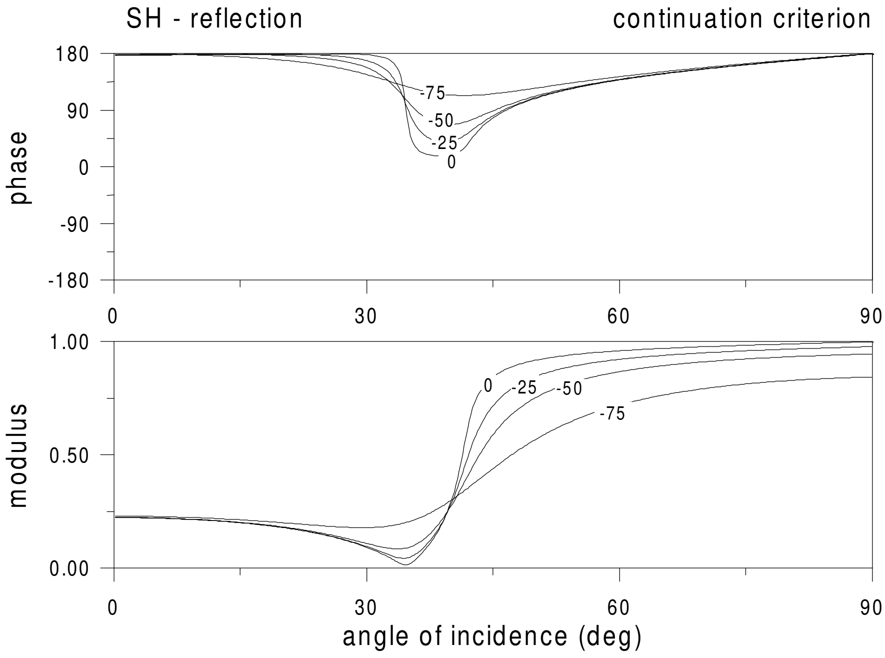

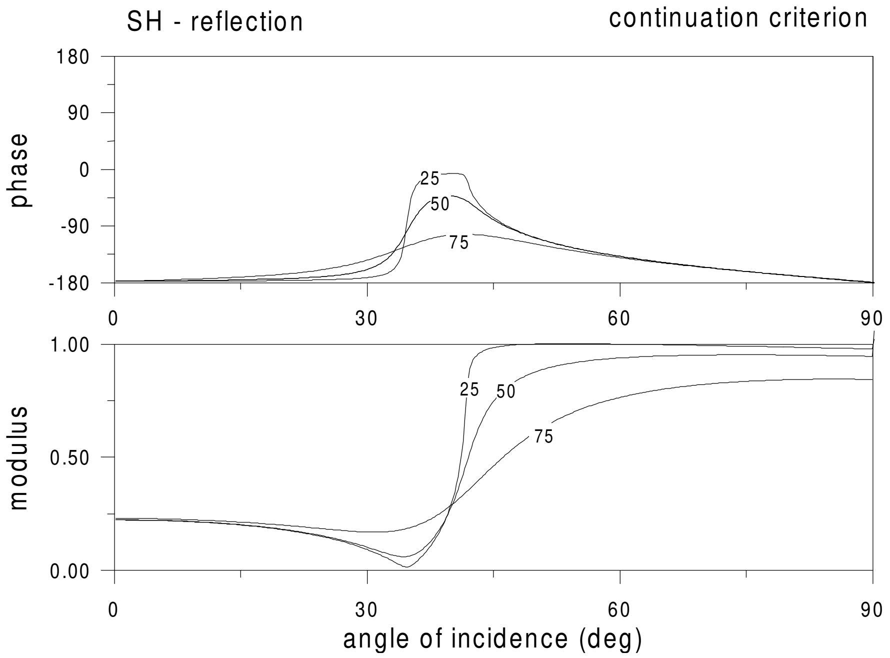

Figure 1: Displacement SH reflection coefficients in MODEL1, for attenuation angles from -75^o to 0^o (top) and from 25^o to 75^o (bottom) with the step of 25^o. The analytic continuation criterion is used to determine the sign of the normal component of the slowness vector of the transmitted wave.

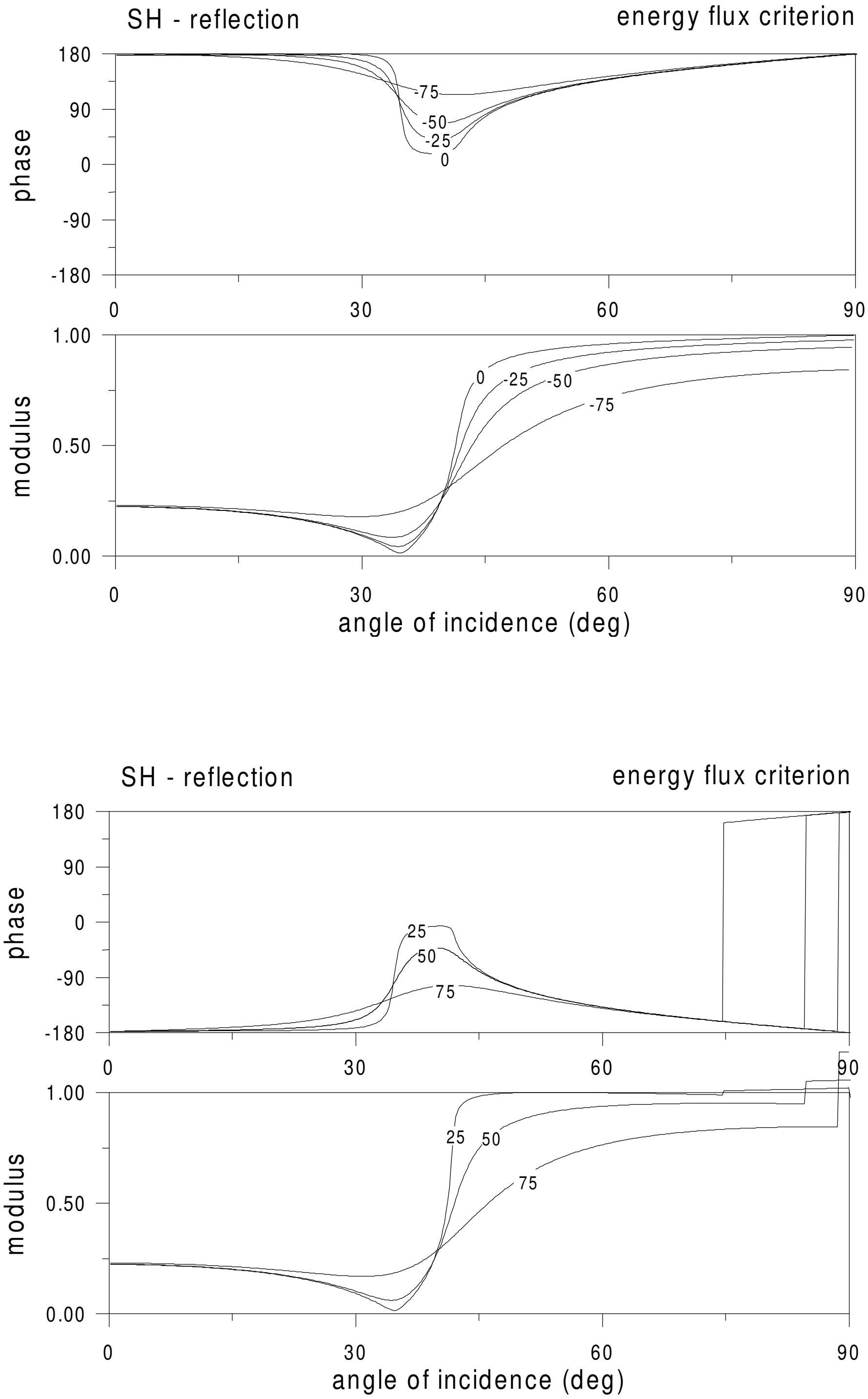

Figure 2: Displacement SH reflection coefficients in MODEL1, for attenuation angles from -75^o to 0^o (top) and from 25^o to 75^o (bottom) with the step of 25^o. The energy flux criterion is used to determine the sign of the normal component of the slowness vector of the transmitted wave. The energy flux criterion requires the downward propagation of energy of the transmitted wave (i.e., the negative normal average energy flux S_3^t). Anomalous jumps in the reflection coefficients are obtained for $\gamma = 25^o, 50^o$, and 75^o.

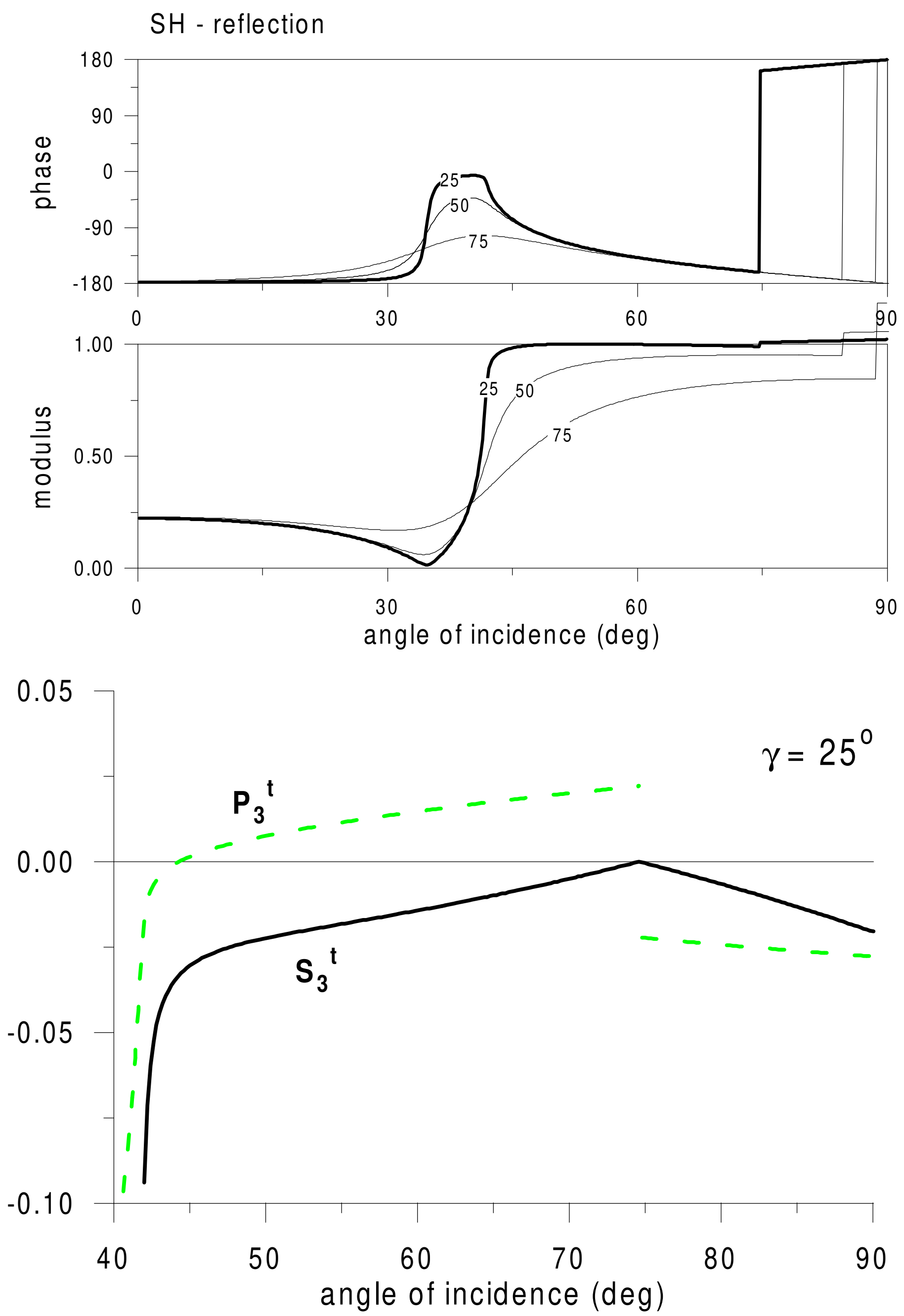

Figure 3: Explanation of the anomalous jumps in the reflection SH coefficients, if the energy flux criterion is used. The bottom figure displays the real part P_3^t of the normal component of the slowness vector p_3^t, and the normal component of the average energy flux S_3^t, both for the transmitted wave, for $\gamma = 25^o$ and for $40^o \leq i \leq 90^o$. The quantities S_3^t are normalized by $|T^{SH}|^2$. For $i = 75^o$, S_3^t vanishes, and for $i > 75^o$, it is necessary to change the sign of p_3^t to keep S_3^t negative. This causes a jump in p_3^t, and, consequently, a jump in the reflection coefficient.

energy flux criterion. In the energy flux criterion, the sign of p_3^t of the transmitted wave is chosen in a such a way to obtain negative normal average energy flux S_3^t (that is, the downward propagation of energy). Both criteria give mostly the same results, particularly for smaller angles of incidence. Only for angles of incidence $> 70^o$, and for the attenuation angles $\gamma = 25^o, 50^o$, and 75^o, the SH reflection coefficients computed with the help of the two criteria are different. See the bottom picture of Fig. 2. The anomalous jumps in the SH reflection coefficients are caused by the application of the energy flux criterion. See a more detailed treatment of the average energy flux criterion in Fig. 3. The bottom picture of Fig. 3, shows P_3^t and S_3^t of transmitted waves, for $\gamma = 25^o$ and for angles of incidence greater than 40^o. (For smaller angles of incidence, no problems appear.) We remind the reader that P_3^t and S_3^t are always negative for transmitted waves in isotropic non-dissipative media. In our case, however, P_3^t=0 for angle of incidence close to 44^o, and is positive for angles of incidence $> 44^o$. Similar situation is, however, common in anisotropic non-dissipative media. From anisotropic non-dissipative media we know that P_3^t may be positive, but S_3^t must be negative (downward propagation of energy). Our situation is, however, even more complicated; as even S_3^t intersects the real axis at $i = 75^o$. In the energy flux criterion, we require that S_3^t is negative for transmitted waves. To fulfill this requirement, it is necessary to change the sign of p_3^t (both P_3^t and A_3^t) for $i > 75^o$, see Fig. 3. This causes the jump in the SH reflection coefficient for the angle of incidence close to 75^o.

5 Behaviour of P_3^t, A_3^t, $\mathrm{Re}F_3^t$, and $\mathrm{Im}F_3^t$

To see the behaviour of the normal components of the slowness vector P_3^t, A_3^t and of the complex Poynting vector $F_3^t = \mathrm{Re}F_3^t + \mathrm{i}\mathrm{Im}F_3^t$ for transmitted waves at the interface Σ in a greater detail, we have calculated them for angles of incidence $0^o \leq i \leq 90^o$, and for the attenuation angles $\gamma = -75^o, -50^o, -25^o, 0^o, 25^o, 50^o$ and 75^o. Note that $\mathrm{Re}F_3^t$ also represents S_3^t, the average energy flux. See Figs. 4a – g. The upper parts of the pictures show these curves in full, the bottom parts of the pictures show the enlarged details. In all pictures, the slowness vector components p_3^t were calculated by the continuation criterion. We are mainly interested in the signs of P_3^t and $\mathrm{Re}F_3^t$. Mostly, these quantities are negative. This corresponds clearly to the downward propagation. For $\gamma = 25^o, 50^o$ and 75^o, however, P_3^t is positive for certain higher angles of incidence. This is not surprising. We can, however, see that even $\mathrm{Re}F_3^t$ are positive for certain angles of incidence close to 90^o. The imaginary parts of the slowness vector (A_3^t) and of the Poynting vector ($\mathrm{Im}F_3^t$) are positive for certain angles of incidence, and negative for other angles of incidence. Thus, $P_3^t, A_3^t, \mathrm{Re}F_3^t$ and $\mathrm{Im}F_3^t$ cannot be directly applied in the local selection criteria.

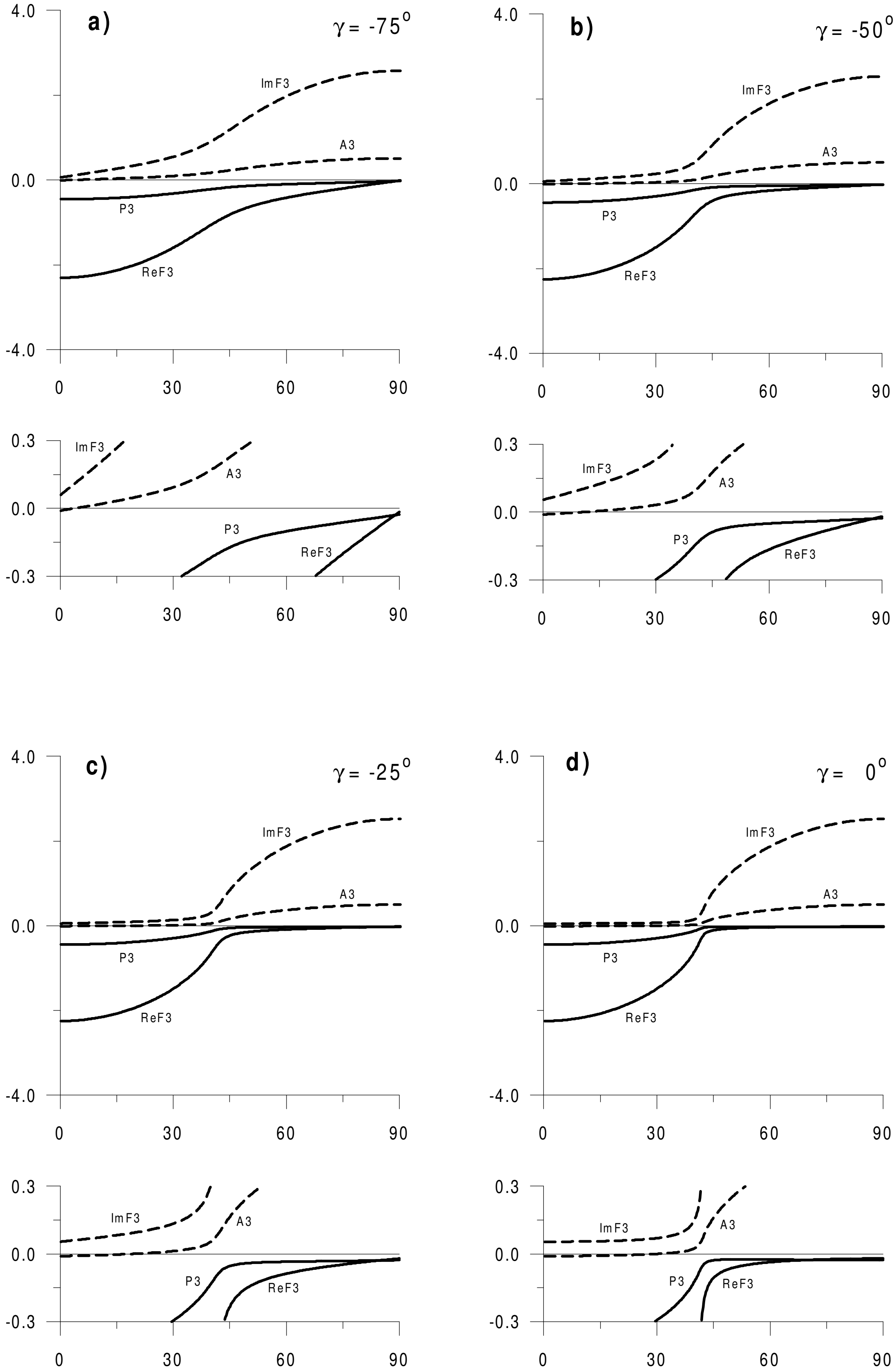

Figure 4: (continued on the next page)

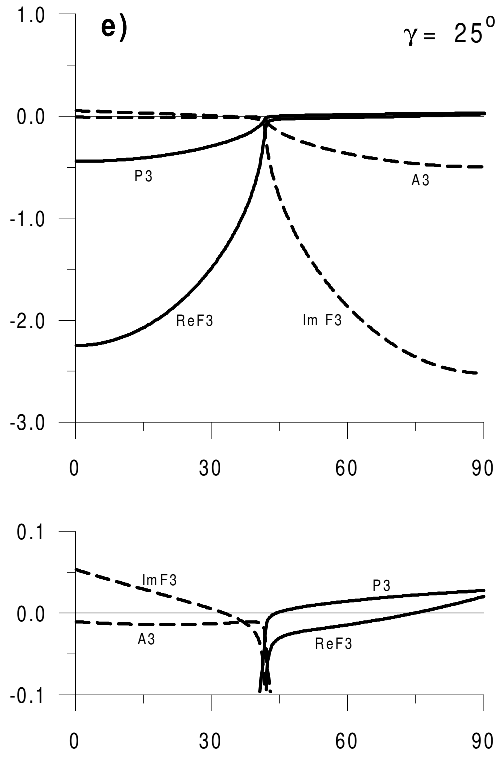

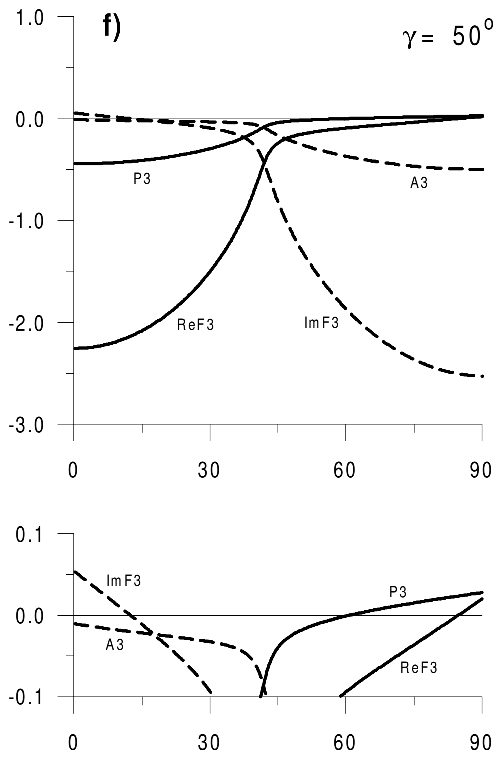

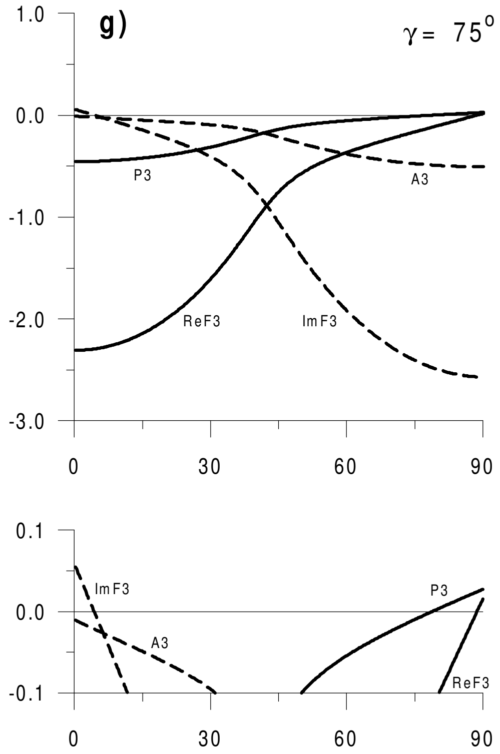

Figure 4: The normal components of the slowness vector $p_3^t = P_3^t + \mathrm{i}A_3^t$, and the normal components of the Poynting vector $F_3^t = \mathrm{Re}F_3^t + \mathrm{i}\mathrm{Im}F_3^t$, for transmitted waves, and for angles of incidence $0^o \leq i \leq 90^o$. Seven different attenuation angles γ are considered: (a) $\gamma = -75^o$, (b) $\gamma = -50^o$, (c) $\gamma = -25^o$, (d) $\gamma = 0^o$, (e) $\gamma = 25^o$, (f) $\gamma = 50^o$, (g) $\gamma = 75^o$. The upper parts of individual pictures show the curves in full, the bottom parts the enlarged details. The symbols P3, A3, ReF3, and ImF3 stand for P_3^t, A_3^t, $\mathrm{Re}F_3^t$, and $\mathrm{Im}F_3^t$, respectively. No one of these quantities is negative for all angles of incidence i and for all attenuation angles γ.

6 Energy conservation equations, instantaneous energy flux

The selection criteria could be also based on the instantaneous energy flux, on the energy conservation equations, on the direction of the exponential decay of amplitudes, or on some other quantities or equations.

In Figs. 5a – 5d and 6a – 6d, we shall present the real and imaginary parts of the instantaneous energy fluxes and of complex Poynting vectors of incident and R/T waves, and the real and imaginary parts of interaction contributions, for angles of incidence $0^o < i < 90^o$, and for the attenuation angle $\gamma = 25^o$. In addition, we also present the energy conservation equations. In Figs. 5a – 5d, the slowness vector of the transmitted wave was computed using the continuation criterion, in Figs. 6a – 6d it was computed using the energy flux criterion. The energy conservation equations correspond to bold lines and are always zero. The energy conservation equations for the Poynting vector contain also the interaction contributions; these interaction contributions are displayed by dashed lines in Figs.5a, 5b, 6a, and 6b.

Let us briefly discuss the interaction contributions. They are small for real parts of energy fluxes, but play a dominant role in the imaginary parts. For great angles of incidence i (say $i > 40^o$ in our case) the imaginary part of the interaction contribution is practically the same as imaginary part of the Poynting vector of the transmitted wave, see Figs. 5d and 6d. They, of course vanish if the instantaneous energy fluxes are considered, see Figs. 5a, 5b, 6a and 6b.

Energy conservation equations should give zero values for all types of energy fluxes used in this paper, see (5), (7), (9). This is strictly confirmed in all pictures, both for real and imaginary parts. The energy conservation equations for the Poynting vector are satisfied only if the appropriate interaction contributions are considered. As explained in Section 3, the interaction contributions need not be considered in the instantaneous energy conservation equations (they vanish in this case).

It is very interesting to see that the energy conservation equations are strictly satisfied not only if the slowness vector is computed by the continuation criterion (see Figs. 5a – 5d), but also if it is computed by the energy flux criterion (see Figs. 6a – 6d). In the latter case, jumps appear in certain curves, but the energy conservation equations are satisfied quite strictly. In certain figures, the jumps are quite dominant, see Figs. 6b and 6d close to 70^o. The consequence is that the energy conservation equations cannot be used in the local selection criteria.

An interesting result, related to the real part of the normal component W_3^t of the instantaneous energy flux of transmitted SH waves was obtained in Fig. 5a. As we can see in Fig. 5a, $\mathrm{Re}W_3^t$ is negative for all angles of incidence in this case. Thus, it would be possible to use $\mathrm{Re}W_3^t$ in the energy based selection criteria in this case. For this reason we paid greater attention to $\mathrm{Re}W_3^t$. We have calculated it for all γ under consideration, see Fig. 7a. Really the result is the same as in Fig. 5a. $\mathrm{Re}W_3^t$ is negative for all angles of incidence and all γ under consideration.

To verify the result, also some other models were treated. In Fig. 7b, we present the result calculated for MODEL2,

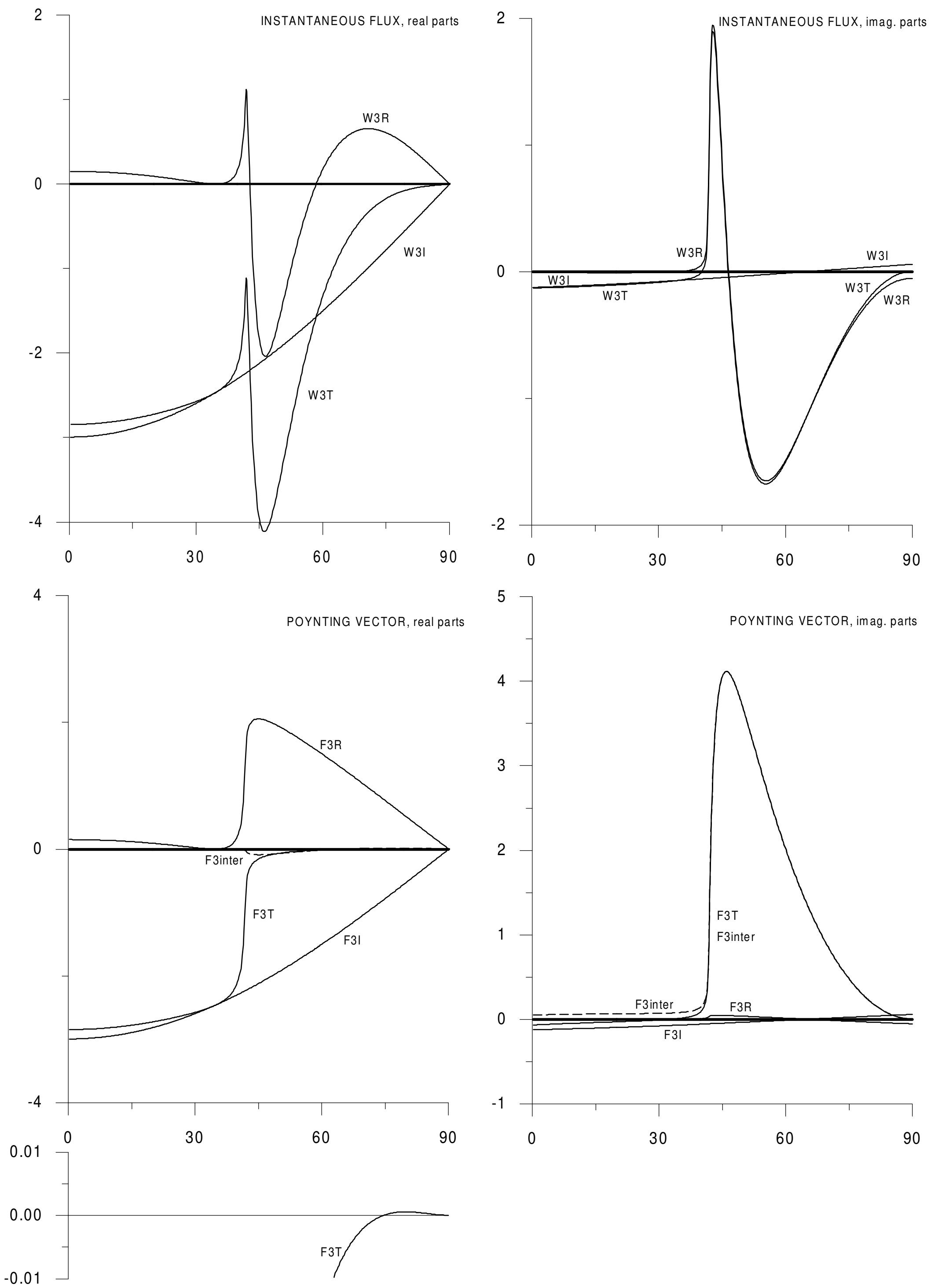

Figure 5: Analytic continuation criterion: the normal components of the instantaneous flux ReW_3 (a), ImW_3 (b) and of the Poynting vector ReF_3 (c), ImF_3 (d) of incident and R/T waves, for $0^o \leq i \leq 90^o$ and $\gamma = 25^o$. In (c), (d), also the interaction contribution F_3^{int} (F3inter) is shown in dashes. Under (c), see an enlarged detail of ReF_3^t. The bold lines (zero in all cases) give the energy conservation at the interface. The notation is self-explanatory (I...incident, R...reflected, T...transmitted wave).

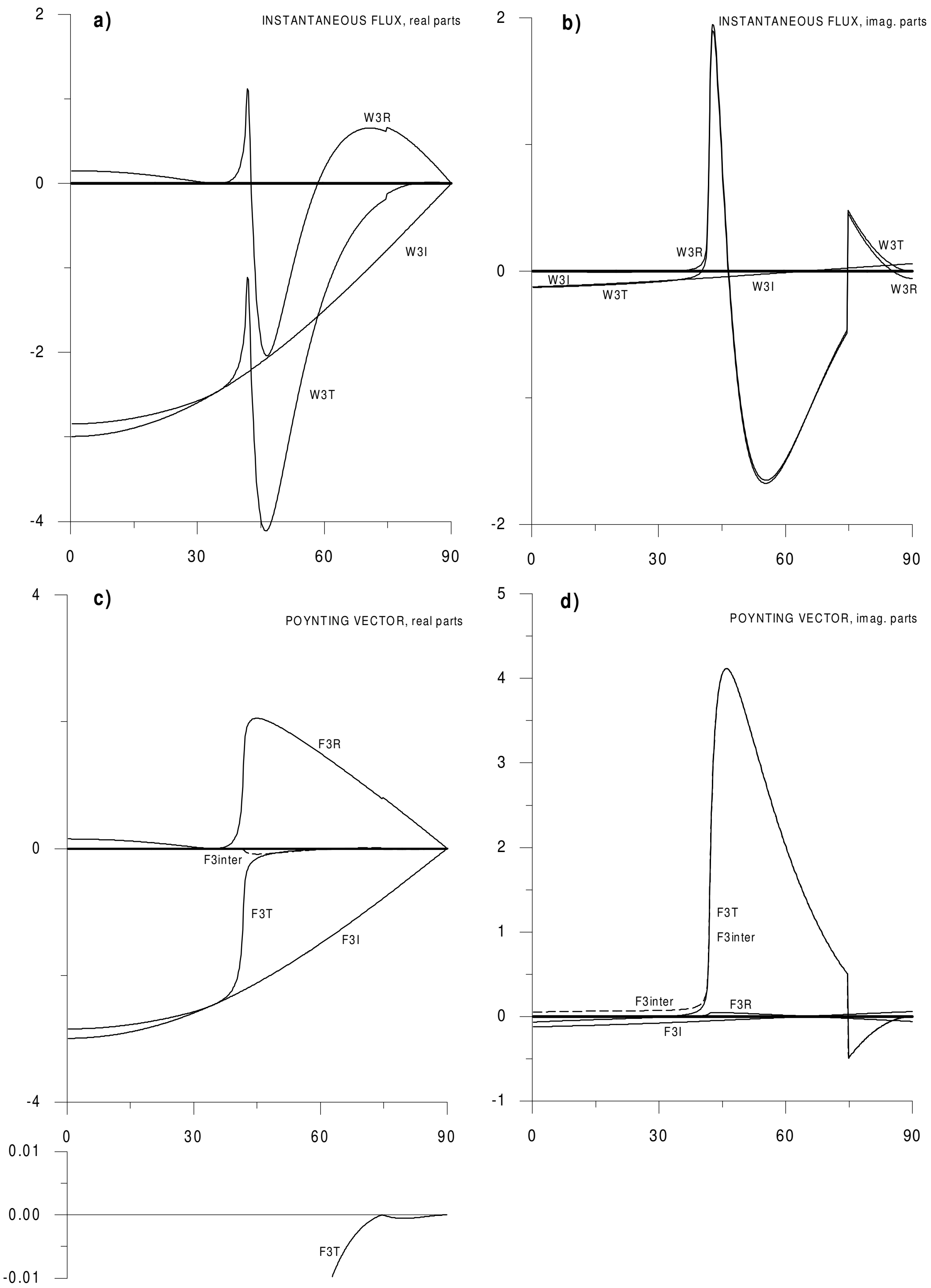

Figure 6: Application of the energy flux criterion. Otherwise, the same quantities as in Fig. 5 are displayed. The anomalous jumps at the angle of incidence $i = 75^o$ are obvious. They are particularly strong in the imaginary parts (see right-hand column). The energy conservation equation is, however, satisfied even in this case; the anomalous jumps do not influence it.

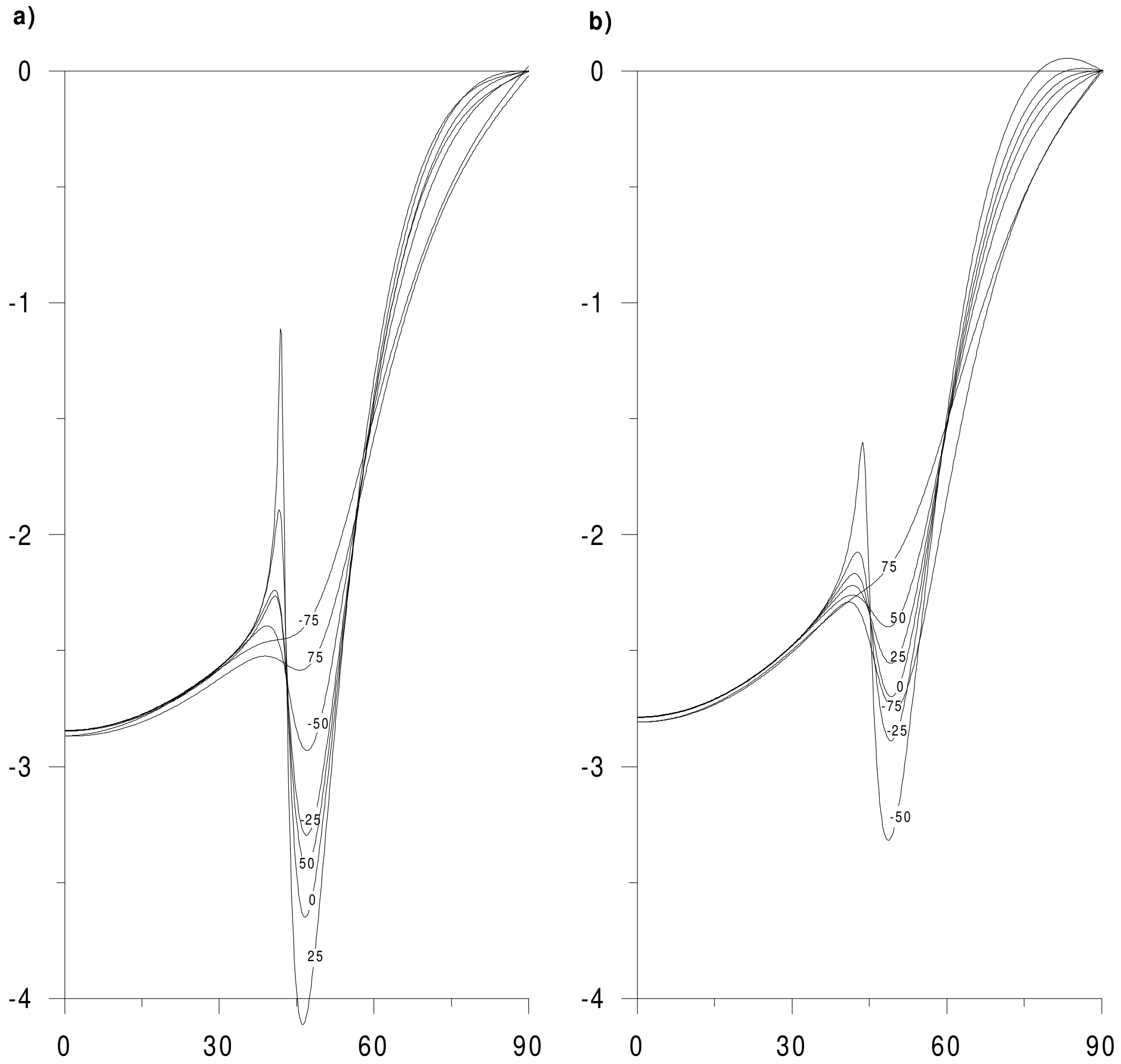

Figure 7: The normal components of the real part of the instantaneous energy flux of the transmitted wave, $\mathrm{Re}W_3^t$, for angles of incidence $0 \leq i \leq 90^o$, and for the attenuation angle $\gamma = -75^o, -50^o, -25^o, 0^o, 25^o, 50^o$, and 75^o. (a) Computation for MODEL1, (b) computation for MODEL2. As we can see, $\mathrm{Re}W_3^t$ is mostly negative, but exceptionally it can also be positive.

$$\begin{array}{ll} \rho_1 = 2.00 \text{ g cm}^{-3}, & \rho_2 = 2.00 \text{ g cm}^{-3}, \\ \beta_1 = 1.44 \text{ km s}^{-1}, & \beta_2 = 2.08 \text{ km s}^{-1}, \\ Q_1 = 13, & Q_2 = 5. \end{array}$$

It can be seen that the quantity $\mathrm{Re}W_3^t$ is also positive for some angles of incidence in this case.

Thus, the real part of the normal instantaneous energy flux cannot be used in the general local selection criteria, either.

7 Special case of $i \leq \gamma$

In this section, we shall consider a special case of the general R/T problem, in which the angle of incidence i is smaller or equal to the attenuation angle γ,

$$i \leq \gamma. \tag{11}$$

In this case, the problem of the selection of correct downgoing and upgoing reflected and transmitted waves can be solved extremely simply.

Let us now consider the dissipative isotropic media. It was shown in Brokešová and Červený (1998, p.29, Eq. (123)) that no critical points exist in the case of $i \leq \gamma$. This implies that the normal component p_3 of the slowness vector can be determined very simply, for any of generated waves,

$$p_3 = \mp \mathcal{P}.\mathcal{V}.[\frac{1}{V_C^2} - a^2]^{\frac{1}{2}}. \tag{12}$$

Here the upper sign (–) corresponds to transmitted waves, the lower sign (+) to reflected waves, $\mathcal{P}$. $\mathcal{V}$. denotes the principal value of the complex square root, a is the tangential component of the slowness vector. (We emphasize that the x_3-axis is pointing into the first medium, containing the incident wave.) The complex valued square of slowness $1/V_C^2$ is given by the relation

$$V_C^{-2} = V^{-2}(1 + Q^{-2})^{-1}(1 + \mathrm{i}Q^{-1}). \tag{13}$$

Here V and Q should be substituted by V_P and Q_P for P waves, and by V_S and Q_S for S waves. They are related to complex-valued Lamé's elastic moduli in dissipative media as follows:

$$\frac{\lambda + 2\mu}{\rho} = V_P^2(1 - \frac{\mathrm{i}}{Q_P}), \quad \frac{\mu}{\rho} = V_S^2(1 - \frac{\mathrm{i}}{Q_S}). \tag{14}$$

It is not difficult to show that the imaginary part of $\mathcal{P}.\mathcal{V}.[1/V_C^2 - a^2]^{\frac{1}{2}}$ is always positive for the normal angle of incidence $i = 0^o$. Then (12) implies that the imaginary part of $\mathcal{P}.\mathcal{V}.[1/V_C^2 - a^2]^{\frac{1}{2}}$ is positive for any angle of incidence satisfying (11). Consequently, we obtain an exponential decay of amplitudes from the interface (both for reflected and transmitted waves).

The condition $i \leq \gamma$ includes a very important and interesting case

$$i = \gamma. \tag{15}$$

Here the angles i and γ again correspond to the incident wave. In this case, the attenuation vector $\mathbf{A}^{inc}$ is perpendicular to the interface, and pointing towards the interface. This implies that the tangential component of the slowness vector $\mathbf{a}$ is real-valued. The consequence is that the tangential components of all generated waves are also real-valued. The normal components p_3 of the slowness vectors of all generated waves can be again determined uniquely using the relation (12). See Fig. 8.

Let us demonstrate these conclusions on our example of SH waves, see MODEL1. Fig. 9 shows the moduli and phases of the SH reflection coefficient for $i = \gamma$. The reflection coefficient behaves smoothly for all angles of incidence $0 \leq i < \frac{1}{2}\pi$. Fig. 10 displays the quantities discussed in Fig. 4, and Fig. 11 the quantities discussed in Fig. 5, versus the angle of incidence, again for $i = \gamma$.

As we have expected, the quantity A_3 for transmitted waves is negative for all angles of incidence, $0 \leq i \leq 90^o$. This corresponds fully to the condition (12). See Fig. 10.

Fig. 11 shows that the energy conservation equations are again satisfied, both for real and imaginary parts of the Poynting vector and of the instantaneous energy flux, for all angles of incidence. We can also observe that the real parts of the normal components of the Poynting vector and of the instantaneous energy flux for transmitted wave are negative for all angles of incidence. Their imaginary parts, however, change signs.

In the **conclusion** it should be emphasized that the case of $i = \gamma$ has certain important advantages over other cases of γ. Let us name several of them. All of them apply to an arbitrary isotropic dissipative medium, with arbitrary quality factor Q.

1. There are no problems with the selection of signs of the normal slowness components p_3 of reflected and transmitted waves. Equation (12) can be used quite universally. Equation (12) yields an exponential decay of amplitudes of all generated waves away from the interface. The application of the continuation criterion is not required, as it is automatically satisfied for $i = \gamma$. Moreover, no energy-based criterion is needed.

2. The requirement that the propagation vector $\mathbf{P}^{inc}$, attenuation vector $\mathbf{A}^{inc}$ and normal $\mathbf{n}$ to the interface be coplanar is always satisfied, as $\mathbf{A}^{inc}$ is parallel to $\mathbf{n}$. This applies even to all generated waves. Consequently, the system of six interface equations for R/T coefficients can be always decomposed into two subsystems for $i = \gamma$, the first (P-SV case) consisting of four equations, and the second (SH case) consisting of two equations.

3. R/T coefficients at a plane interface between two isotropic dissipative media depend only weakly on γ for moderate angles of incidence i (even for $i \neq \gamma$), see Brokešová and Červený (1998). Consequently, the specification $\gamma = i$ can be used safely even in the AVO and AVA analysis. Only for greater angles of incidence, the variations due to γ may be more pronounced.

4. For $i = \gamma$, the phases of R/T coefficients in dissipative media (Q finite) approach always the phases of relevant R/T coefficients in non-dissipative media ($Q = \infty$), if $Q \rightarrow \infty$. This is not the case for arbitrarily chosen $\gamma \neq i$, where the limiting case $Q \rightarrow \infty$ may yield the opposite signs of phases of R/T coefficients. See Brokešová and Červený (1998, p. 24, §5e).

5. There are no additional difficulties in the computation of R/T coefficients at an dissipative transition layer (composed from parallel dissipative isotropic sublayers). The attenuation vector $\mathbf{A}$ remains vertical in all sublayers of the layer. In other words, the lateral slowness components are real-valued throughout the transition layer. Consequently,

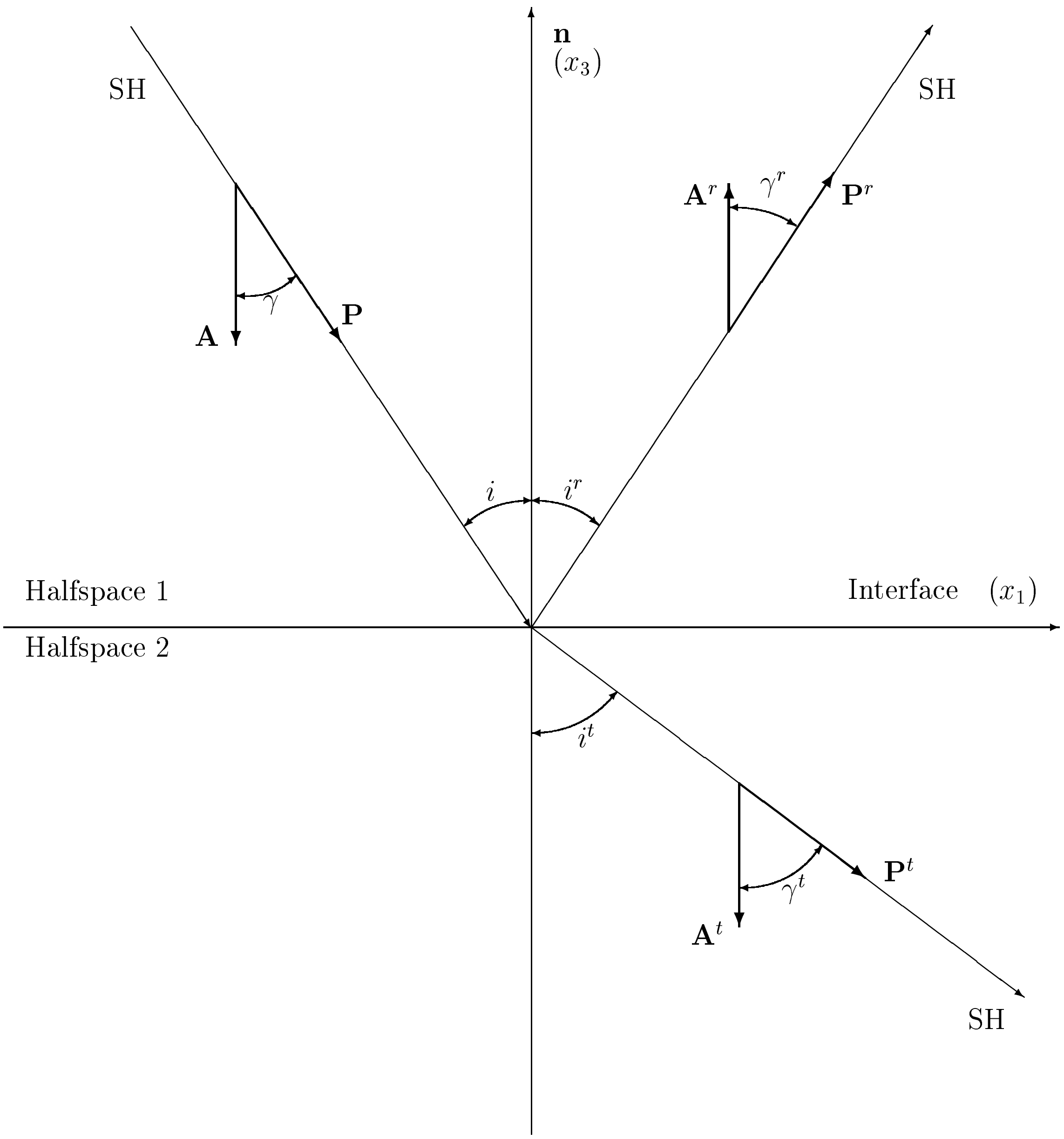

Figure 8: Reflection and transmission of an inhomogeneous plane SH wave with $i = \gamma$ on a plane interface between two isotropic dissipative halfspaces (schematically). As $i = \gamma$, the attenuation vector $\mathbf{A}$ of the incident wave is parallel to the x_3-axis. In this case, the attenuation vectors of reflected and transmitted waves ($\mathbf{A}^r$ and $\mathbf{A}^t$) are also parallel to the x_3-axis.

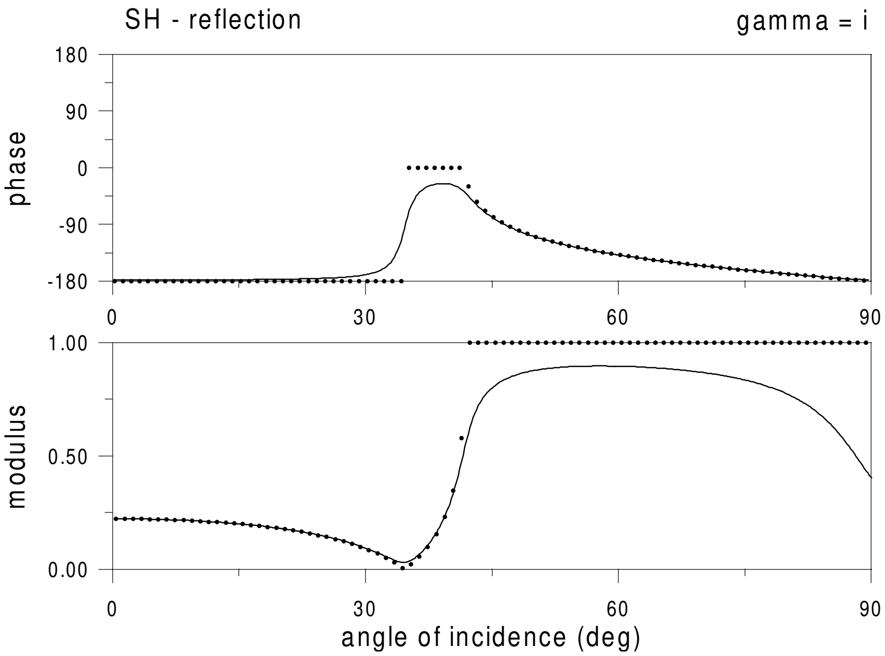

Figure 9: Displacement SH reflection coefficients in MODEL1, for the attenuation angle γ equal to the angle of incidence i, $i = \gamma$. The relevant SH reflection coefficient for a non-dissipative medium is displayed by a dotted curve.

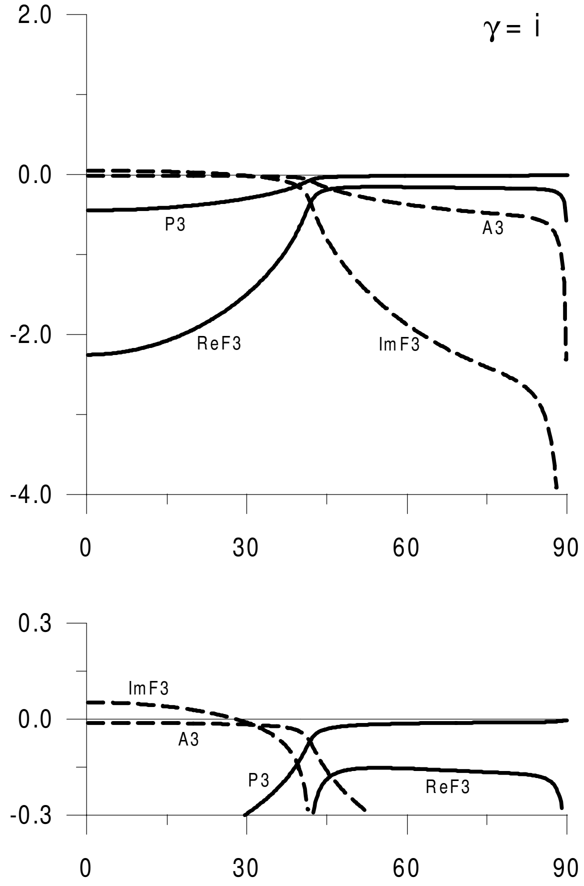

Figure 10: Dtto as in Fig. 4, but for $\gamma = i$. The quantities A_3^t, P_3^t and $\mathrm{Re}F_3^t$ are negative for all angles of incidence i in this case.

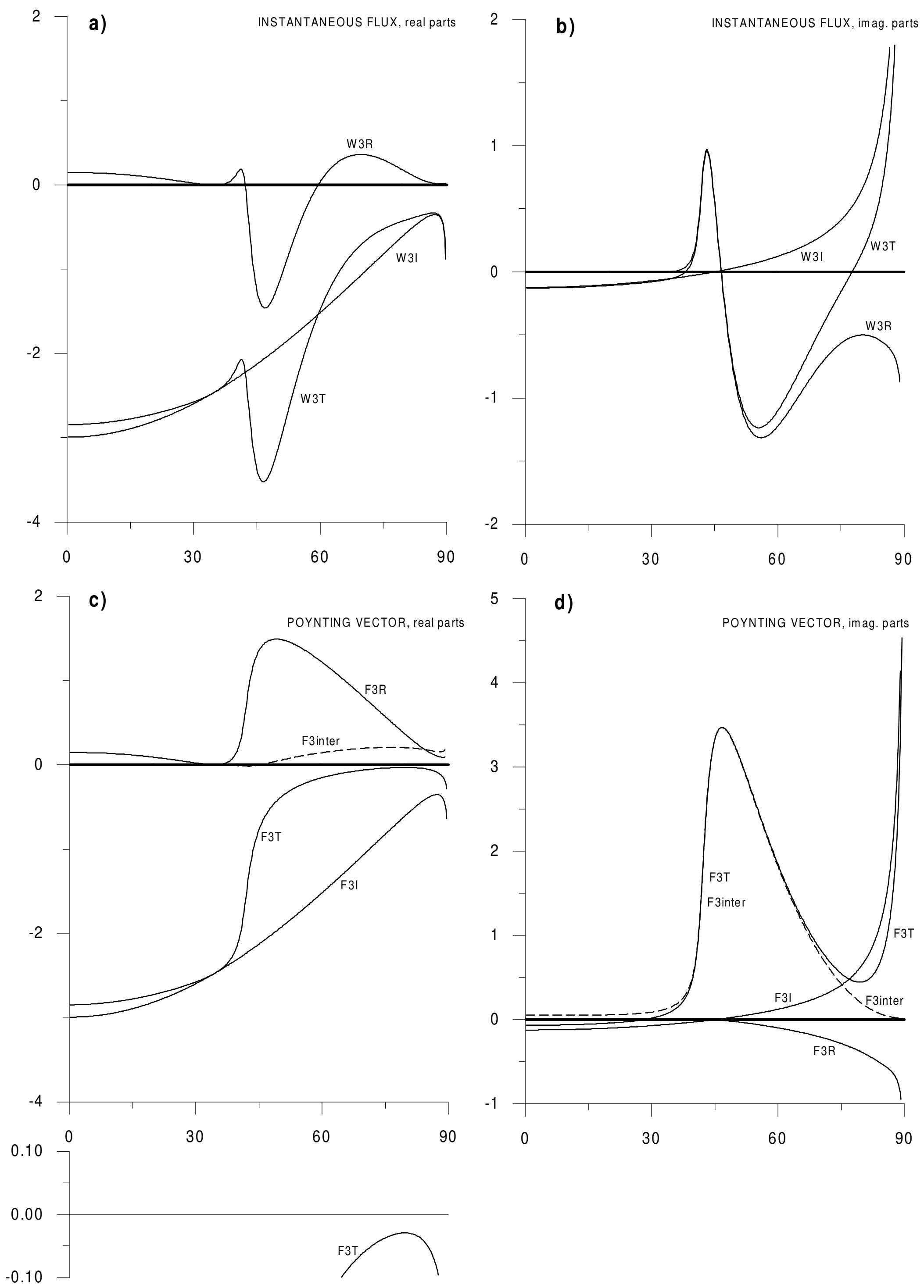

Figure 11: Dtto as in Fig. 5, but for $\gamma = i$. The quantities $\mathrm{Re}W_3^t$ (denoted by W3T in (a)) and $\mathrm{Re}F_3^t$ (denoted by F3T in (c)) are negative for all angles of incidence i in this case.

the computer program COEF52 (described in Brokešová and Červený, 1998) may be safely used to compute the R/T coefficients at a transition layer between two dissipative isotropic halfspaces, where even the sublayers of the transition layer may be dissipative. It is only necessary to specify $i = \gamma$ for the incident wave, or, in other words, specify lateral slowness components to be real-valued.

Finally, a note to anisotropic dissipative media. Analogous approach can be safely used even if we compute the R/T coefficients at a plane interface between two anisotropic dissipative media, or at a transition layer between two anisotropic dissipative media. The individual sublayers in the transition layer may also be anisotropic dissipative. We have to consider real-valued p_1, p_2 for the incident wave. Then p_1 and p_2 are constant and real-valued throughout the whole layer and across the interface(s). The selection of correct eigenvalues p_3 corresponding to reflected and transmitted waves is also straightforward in this case.

Acknowledgement

The research has been supported by the consortium project "Seismic Waves in Complex 3-D Structures".

References

Ainslie, M. A., and Burns, P. W. (1995). Energy conserving reflection and transmission coefficients for a solid-solid boundary. *J. Acoust. Soc. Am* **98**, 2836 – 40.

Auld, B. A. (1973). *Acoustic fields and waves in solids.*, New York: Wiley-Interscience.

Brokešová, J. (in press). Reflection/transmission coefficients at a plane interface in dissipative and non-dissipative isotropic media: a comparison. *Journal of Computational Acoustics.*

Brokešová, J., and Červený, V. (1998). Inhomogeneous plane waves in dissipative, isotropic and anisotropic media. Reflection/transmission coefficients. In *Seismic waves in complex 3-D structures*, Report 7, pp. 57 – 146. Prague: Charles Univ., Faculty of Mathematics and Physics, Dept. of Geophysics.

Burridge, R. (1976). *Some mathematical topics in seismology.* New York: New York Univ., Courant Inst. of Math. Sci.

Červený, V. (2001a). *Seismic ray theory.* New York: Cambridge Univ. Press

Červený, V. (2001b). Reduced Hamiltonian in ray tracing systems for anisotropic inhomogeneous media. In *Seismic waves in complex 3-D structures*, this report.

Červený, V. (2001c). Energy flux of time-harmonic waves in anisotropic dissipative media. In *Seismic waves in complex 3-D structures*, this report.

Deschamps, M. (1990). Réflexion-réfraction de l'onde plane hétérogène: Repartition de l'énergie. *J. Acoust.* **3**, 251 – 61.

Krebes, E. S. (1984). On the reflection and transmission of viscoelastic waves — Some numerical results. *Geophysics* **49**, 1374 – 80.